



## D5.1 – REPORT ON THE DESIGN AND FABRICATION ISSUES OF THE OPTICAL GRATING

StretchBio – D5.1

Identifier:	StretchBio_D.5.1_Report on the design and fabrication issues of the optical grating
Work package:	WP 5
Dissemination level:	Public
Keywords:	Grating, coupling, finite-difference-time-domain-method
Abstract:	This deliverable presents the results of the simulation of grating coupler designs on an SOI platform to efficiently couple light from a single-mode fiber into a low-loss single-mode waveguide and the upcoming fabrication challenges, especially with regards to fabrication compatibility with the photonic crystal device. It reports the coupling efficiencies and bandwidths of different coupler designs depending on the wavelength to address, which is given by working in air or water. It also includes the design of an adiabatic linear taper for efficient mode-field matching from a single-mode fiber (mode-field diameter of roughly 10 $\mu\text{m}$ ) to a single-mode waveguide (500 x 400 $\text{nm}^2$ ).

## Document history:

Version	Date	Reason of change
1	14/07/2022	Creation of document
1.1	22/07/2022	First draft
1.2	25/08/2022	First revision
1.3	29/08/2022	Second version
1.4	30/08/2022	Final version

## Document author(s):

Entity	Contributor
ALU	Jens Goldschmidt
ALU	Katrin Schmitt
UB-IN2UB	Albert Romano-Rodriguez
UB-IN2UB	Francisco Hernández-Ramírez
UB-IN2UB	Elena Lopez-Aymerich
DTU	Christian Vinther Bertelsen

## Disclosure Statement:

This document has been produced by consortium partners of the *StretchBio* Horizon 2020 project, funded by the European Union's Horizon 2020 research and innovation programme under grant agreement No. 964808. The content of this document, the information contained herein, and the views expressed are those of the authors and do not necessarily reflect the official opinion of the European Union. Neither the European Union institutions and bodies nor any person acting on their behalf may be held responsible for the use which may be made of the information contained.

## Executive Summary

---

This deliverable presents the results of the simulation of grating coupler designs on a silicon-on-insulator (SOI) platform to efficiently couple light from a single-mode fiber into a low-loss single-mode waveguide and the upcoming fabrication challenges, especially with regards to fabrication compatibility with the photonic crystal device. It reports the coupling efficiencies and bandwidths of different coupler designs depending on the wavelength to address, which is given by working in air or water. It also includes the design of an adiabatic linear taper for efficient mode-field matching from a single-mode fiber (mode-field diameter of roughly 10  $\mu\text{m}$ ) to a single-mode waveguide (500 x 400  $\text{nm}^2$ ).

The obtained grating design parameters give the needed specifications for the fabrication of a coupler to efficiently guide light into the photonic crystal sensor device proposed in StretchBio.

# Table of Contents

<b>EXECUTIVE SUMMARY .....</b>	<b>3</b>
<b>1 INTRODUCTION .....</b>	<b>6</b>
1.1 PURPOSE OF THE DOCUMENT .....	6
1.2 SCOPE OF THE DOCUMENT .....	6
1.3 RELATED DOCUMENTS .....	7
<b>2 GRATING COUPLERS .....</b>	<b>8</b>
2.1 THEORY .....	8
2.2 DESCRIPTION OF MODEL SETUP .....	9
<b>3 RESULTS.....</b>	<b>11</b>
3.1 GRATING OPTIMIZATION.....	11
3.1.1 PERIOD AND FILL FACTOR.....	11
3.1.2 BANDWIDTH OPTIMIZATION .....	12
3.2 DESIGN OF THE ADIABATIC TAPER .....	14
3.3 COMPATIBILITY WITH FABRICATION ROUTE.....	16
3.3.1 INFLUENCE OF VARIATION IN SI THICKNESS.....	16
<b>4 CONCLUSIONS AND FUTURE WORK .....</b>	<b>18</b>
<b>GLOSSARY.....</b>	<b>19</b>

## List of Figures

Figure 1: Schematic of a grating coupler to couple light from a single-mode fiber into a single-mode SOI waveguide with an adiabatic linear taper .....	8
Figure 2: Simulation setup to optimize grating dimensions .....	9
Figure 3: Simulation domain for the design of the adiabatic taper .....	10
Figure 4: Simulated coupling efficiencies over wavelength for the optimized grating structure in air, in water and in water where air is still present in the grating trenches.....	12
Figure 5: Coupling spectra for different linear grating chirps ranging from 10 to 50 nm for the first coupling scenario. ....	13
Figure 6: Coupling spectra for different linear grating chirps ranging from 10 to 50 nm for the second coupling scenario. ....	14
Figure 7: Coupling spectra for different linear grating chirps ranging from 10 to 50 nm for the third coupling scenario. ....	14
Figure 8: Transmission through the linear taper for operation in air with a target wavelength of 1.53 $\mu\text{m}$ and in water with a target wavelength of 1.38 $\mu\text{m}$ along with the corresponding fitted curves. ....	15
Figure 9: 3D-simulation setup with a taper length of 30 $\mu\text{m}$ for better clarity.....	15
Figure 10: Coupling spectra for different Si thicknesses ranging from 300 to 500 nm for the first coupling scenario. ....	16
Figure 11: Coupling spectra for different Si thicknesses ranging from 300 to 500 nm for the second coupling scenario. ....	17

## List of Tables

Table 1: Simulation results of grating optimization for a grating in air (wavelength of 1.53 $\mu\text{m}$ ), a grating in water (wavelength of 1.38 $\mu\text{m}$ ) and a grating in water in which the grating trenches are filled with air (wavelength of 1.38 $\mu\text{m}$ ).....	11
Table 2: Simulation results of linear chirped grating optimization for the three cases.....	13

# 1 Introduction

---

## 1.1 Purpose of the document

This report is the first deliverable for WP5 (D5.1) of the StretchBio project, and presents the theoretical results of coupling efficiencies and bandwidths for different grating coupler designs working with different elements; from a standard single-mode silica fiber to a silicon single-mode waveguide structure on an SOI platform. For details on the overall purpose, we refer to the project description given in the grant agreement.

The final coupling device will be able to efficiently couple light in the near-infrared range into the silicon waveguide. To optimize the coupling efficiency and enhance the optical bandwidth of the coupler to the photonic crystal device while adjusting to the infrared wavelength, we have used simulation tools for guiding towards the appropriate coupler designs. These devices will be fabricated in later steps of the project.

The deliverable gives an overview of the principles of grating couplers and which parameters have to be tuned to enhance coupling efficiency and bandwidth. So, the following questions are addressed in this report:

- How does the coupling efficiency depend on the grating period and on the grating fill-factor?
- How can the coupling bandwidth be increased?
- How does the grating coupler behave in different environments (e.g. grating in air or in water)?
- How will fabrication uncertainties (e.g., deviations from expected silicon thickness) influence light coupling?
- How can efficient mode-field conversion from a single-mode fiber to a single-mode silicon waveguide be achieved?
- How does the grating fabrication fit in the overall fabrication route?

Therefore, we used Maxwell's equations in dielectric media and the finite-difference-time-domain method simulation tool *MEEP*<sup>1</sup> as well as the wave-optics module of *COMSOL Multiphysics*<sup>2</sup> to answer the above questions.

The simulation models developed can be used in the future to simulate other coupler geometries that might need to be required at later stages of the project.

## 1.2 Scope of the document

This deliverable includes:

- A brief overview of the working principle of grating couplers;

---

<sup>1</sup> A. Oskooi et al., "MEEP: A flexible free-software package for electromagnetic simulations by the FDTD2 method," *Computer Physics Communications* 181, 687-702 (2010), doi: [10.1016/j.cpc.2009.11.008](https://doi.org/10.1016/j.cpc.2009.11.008)

<sup>2</sup> COMSOL website (<https://www.comsol.com/>). Last search: August 25<sup>th</sup> 2022.

- A discussion and demonstration of simulation results for the effect of different grating periods and fill factors on the coupling efficiency for different wavelengths in air and water environment;
- A discussion and demonstration of simulation results for the effect on the coupling bandwidth by introducing a grating chirp;
- A discussion and demonstration of simulation results for different waveguide taper geometry for matching the in-coupled mode to the waveguide mode;
- A discussion of fabrication challenges regarding the compatibility to the photonic crystal fabrication route.

In this report, we show that a grating period of 0.56  $\mu\text{m}$  with a fill factor of 90 % (90 % silicon, 10 % air) for a target wavelength of 1.53  $\mu\text{m}$ , which is given by the design of the photonic crystal structure in air, shows a coupling efficiency of 13 % for vertical coupling. This results in a coupler bandwidth of 17 nm.

To increase the bandwidth, we introduce a linear chirp of the grating period by 50 nm while keeping the width of the air gap constant, which slightly reduces the maximum coupling efficiency, but the bandwidth is increased to 96 nm. In water, the target wavelength is 1.38  $\mu\text{m}$  and we find an optimum grating period of 0.5  $\mu\text{m}$  with a fill factor of 90 % (90 % silicon, 10 % water), which results in maximum coupling efficiency of 38 % and a bandwidth of 56 nm. By introducing a linear chirp of 10 nm the maximum coupling efficiency is decreased to < 30 % by increasing the bandwidth to 95 nm. At the current stage of the project, we still consider the possibility that the grating trenches will be filled with water. For that case, we show the coupling behavior in water where there is still air in the grating trenches. This results in a decreased coupling efficiency of 20 %.

We also show the optimum length of a linear taper to match the wide single-mode fiber mode to the narrow waveguide mode. Lastly, we briefly discuss the influence of varying silicon thicknesses on the coupling performance

### 1.3 Related documents

This report provides important information for the fabrication of coupling structures to be able to efficiently couple light from a standard silica single-mode fiber into the photonic crystal sensor. To obtain a comprehensive view of the StretchBio project and the work presented here, the reading of the deliverables of WP2 and WP3 can be helpful.

## 2 Grating couplers

In this section the basic working principles and theory of grating couplers are introduced as well as a description of the simulation setup.

### 2.1 Theory

A grating is a periodic or non-periodic arrangement of materials with different refractive indices. On the SOI-based platform used in this project, gratings will be realized by etching trenches into the silicon. This leads to diffraction of incident light into different directions. If the grating is on the surface of a light guiding structure (waveguide), light can be coupled into that structure if the phase matching conditions are met, which are given by the Bragg condition<sup>3</sup>

$$\frac{2\pi n}{\lambda_0} \sin \theta + m \frac{2\pi}{\Lambda} = \beta_m.$$

Here,  $n$  is the refractive of the medium between the fiber and the grating,  $\lambda_0$  the vacuum wavelength,  $\theta$  the angle to the normal of the grating structure,  $\Lambda$  the grating period and  $\beta_m$  the propagation constant in the grating for a specific diffraction order  $m$ . Typically,  $\beta_m$  is unknown and, so, one has to use numerical techniques in order to find the ideal  $\Lambda$  for efficient coupling.

Figure 1 shows a typical schematic setup for grating coupling. To minimize losses in the waveguide it is favorable to use single-mode waveguides, which typically have widths and heights from 300 to 500 nm in the targeted wavelength regime of 1.35 to 1.55  $\mu\text{m}$ . However, single-mode fibers have typical diameters of 10  $\mu\text{m}$ , so one has to use spot converters. This is realized by using so-called adiabatic tapering, where the waveguide width is slowly linearly decreased while maintaining single-mode operation if the condition

$$\theta_{taper} < \frac{\lambda_0}{2Wn_{eff}}$$

is satisfied. Here is  $\theta_{taper}$  the half-angle of the taper,  $W$  the varying waveguide width in direction of propagation and  $n_{eff}$  is the effective index of the mode for a specific width<sup>3</sup>.

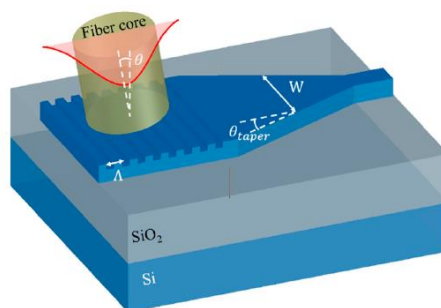


Figure 1: Schematic of a grating coupler to couple light from a single-mode fiber into a single-mode SOI waveguide with an adiabatic linear taper<sup>3</sup>

<sup>3</sup> L. Cheng et al., "Grating Couplers on Silicon Photonics: Design Principles; Emerging Trends and Practical Issues," *Micromachines* 11 (2020), doi: [10.3390/mi11070666](https://doi.org/10.3390/mi11070666)

## 2.2 Description of model setup

For the grating simulation we implemented a Finite-Difference Time Domain (FDTD) model, in which we assumed lossless light propagation in the media with no birefringence. We then implemented a 2D simulation domain of a size of  $27 \times 6 \mu\text{m}^2$  with a resolution of 20 nm, where  $1 \mu\text{m}$  thick perfectly matched layers (PML) were introduced at the edges<sup>4</sup>.

Figure 2 shows an exemplary simulation domain. The 400 nm thick grating and waveguide structures in silicon sit on a  $1 \mu\text{m}$  thick  $\text{SiO}_2$  layer on top of infinitely thick bulk silicon. The grating is etched completely through the silicon to the oxide to be compatible with the fabrication route of the whole sensor device. A gaussian beam source is implemented roughly  $1 \mu\text{m}$  above the grating structure representing the single-mode fiber tip with a mode field diameter of  $10.4 \mu\text{m}$ . The source is polarized TM-like (E-field in x-direction), which is necessary for the planned photonic crystal device to show a complete photonic band gap<sup>4</sup>.

In a first iteration the grating period along with the fill factor of the grating were changed from 0.3 to  $1 \mu\text{m}$  and from 10% to 90%, respectively, for operation in air (target wavelength of  $1.53 \mu\text{m}$ ) and in water (target wavelength of  $1.38 \mu\text{m}$ ) in order to optimize the coupling efficiency for a coupling angle of  $0^\circ$ . An angle of  $0^\circ$  was chosen for easier alignment in a real device, because in later stages of the project multiple devices will be addressed at once with an array of fibers. We then analyzed the bandwidth of the found grating parameters and introduced a chirped part into the grating, where the grating period was varied to increase the coupling bandwidth.

To test the optimum length of the adiabatic taper we setup a 2D model in *COMSOL Multiphysics*. A  $12 \mu\text{m}$  wide silicon waveguide surrounded by air/water where the width is linearly decreased to 500 nm to maintain single-mode operation was used. We then iterated through taper lengths of 10 to  $500 \mu\text{m}$  and calculated the transmission.

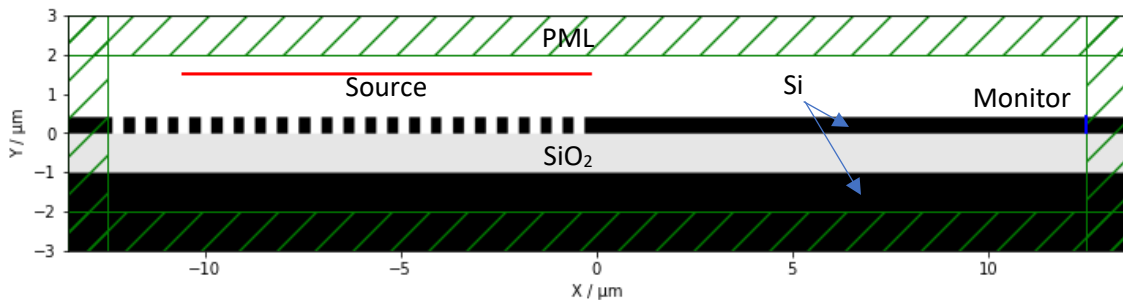


Figure 2: Simulation setup to optimize grating dimensions. The grating and the waveguide structure sit on a  $1 \mu\text{m}$  thick buried silicon dioxide layer on bulk silicon in air.

Figure 3 shows the simulation domain for an exemplary taper length of  $30 \mu\text{m}$ .

<sup>4</sup>J. D. Joannopoulos et al., "Photonic Crystals: Molding the Flow of Light 2<sup>nd</sup> Edition," Princeton University Press (2008)

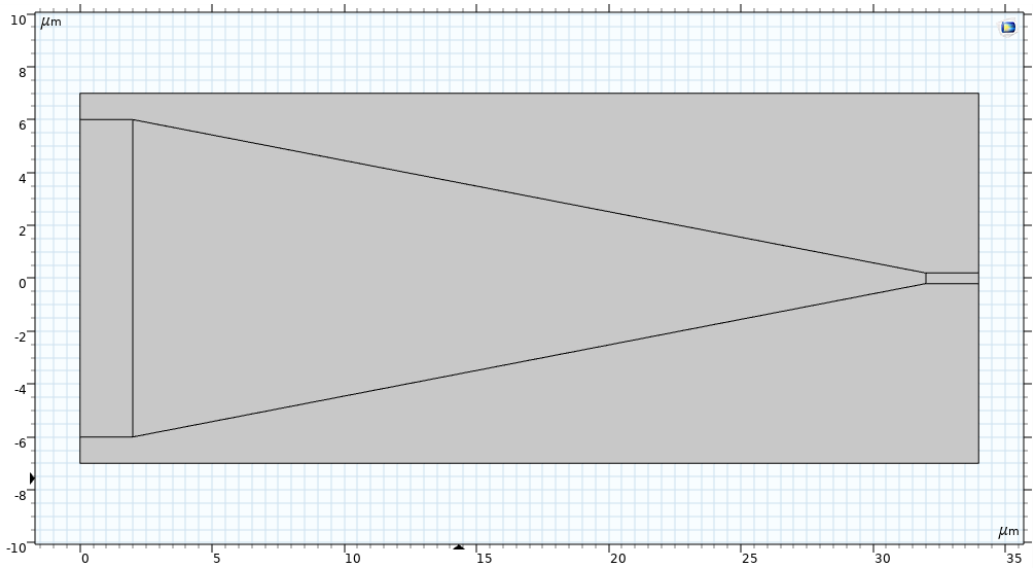


Figure 3: Simulation domain for the design of the adiabatic taper.

## 3 Results

---

Several simulations to investigate the dimensions of the gratings to optimize coupling efficiency and bandwidth, as well as the conversion efficiency of the implemented adiabatic taper, were performed.

For the grating simulations, we used *MEEP* version 1.17.1 on a desktop computer, running Windows 10. The simulations of the adiabatic taper were performed on a Windows Server 2016 running the wave-optics module of *COMSOL Multiphysics* 6.0.

### 3.1 Grating optimization

#### 3.1.1 Period and fill factor

The coupling efficiencies for grating periods of a one-dimensional grating were tested in a range between 0.3  $\mu\text{m}$  and 1  $\mu\text{m}$  in 10 nm steps, while the fill factors were changed from 10 to 90% in 10% steps. Also, we tested the needed number of grating periods between 15 and 25 for the highest coupling efficiency. These numbers lie in a range which is typically found in literature, e.g., in Dabos et al.<sup>5</sup>

All materials were treated as isotropic with no birefringence. The refractive indices of the materials for different wavelengths were selected from Schinke et al.<sup>6</sup> for silicon and from Malitson et al.<sup>7</sup> for  $\text{SiO}_2$ . For air we assumed a refractive index of 1 and for water, 1.32.<sup>8</sup>

Table 1 shows the optimized grating parameters and the resulting coupling efficiencies and bandwidths for a grating with 22 periods in air with a target wavelength of 1.53  $\mu\text{m}$  (scenario 1) and for a grating in water with a target wavelength of 1.38  $\mu\text{m}$  (scenario 2). As the grating trenches themselves will most likely not be filled with water, we also simulated the coupling behavior, where the trenches are filled with air and water is on top of the structure (scenario 3).

*Table 1: Simulation results of grating optimization for a grating in air (wavelength of 1.53  $\mu\text{m}$ ), a grating in water (wavelength of 1.38  $\mu\text{m}$ ) and a grating in water in which the grating trenches are filled with air (wavelength of 1.38  $\mu\text{m}$ ).*

Scenario	Period / $\mu\text{m}$	Fill-factor / %	Optimized coupling efficiency / db (%)
1	0.56	90	-8.74 (13.36)
2	0.5	90	-4.26 (37.50)
3	0.5	90	-6.90 (20.42)

---

<sup>5</sup> G. Dabos et al., "Perfectly vertical and fully etched SOI grating couplers for TM polarization," *Opt. Com.* 124-127 (2015), doi: [10.1016/j.optcom.2015.03.081](https://doi.org/10.1016/j.optcom.2015.03.081)

<sup>6</sup> C. Schinke et al., "Uncertainty analysis for the coefficient of band-to-band absorption of crystalline silicon," doi: [10.1063/1.4923379](https://doi.org/10.1063/1.4923379)

<sup>7</sup> I. H. Malitson et al., "Interspecimen comparison of the refractive index of fused silica," *J. Opt. Soc. Am.* 55, 1205-1208 (1965), doi: [10.1364/JOSA.55.001205](https://doi.org/10.1364/JOSA.55.001205)

<sup>8</sup> S. Kedenburg et al., "Linear refractive index and absorption measurements of nonlinear optical liquids in the visible and near-infrared spectral region," *Opt. Mat. Express* 2, 1588-1611 (2012), doi: [10.1364/OME.2.001588](https://doi.org/10.1364/OME.2.001588)

It can easily be seen that if air remains in the grating trenches while coupling in the water environment, the coupling efficiency is lowered by more than 2 dB. This behavior will be further investigated in the next steps of the project on fabricated gratings by performing contact angle measurements on the grating structure to verify if water will be present in between the grating teeth.

It has to be mentioned that the coupling efficiencies can be increased by slightly tilting the fiber. For example, for scenario 1 the coupling efficiency is -7.12 dB (19.41%) for a tilt angle of 15°. However, as mentioned before we want to abstain from doing this for the ease of use when we want to address different structures with several fibers at once.

### 3.1.2 Bandwidth optimization

To analyze the bandwidth of the grating coupler a pulse was launched from the gaussian source to excite wavelengths from 1.25  $\mu\text{m}$  to 1.65  $\mu\text{m}$ . The bandwidths were derived from the wavelengths where the coupling efficiency drops -3 dB from the maximum achieved efficiency in the targeted wavelength region. Figure 4 shows the coupling efficiency spectra for the three earlier described scenarios and the respective grating parameters.

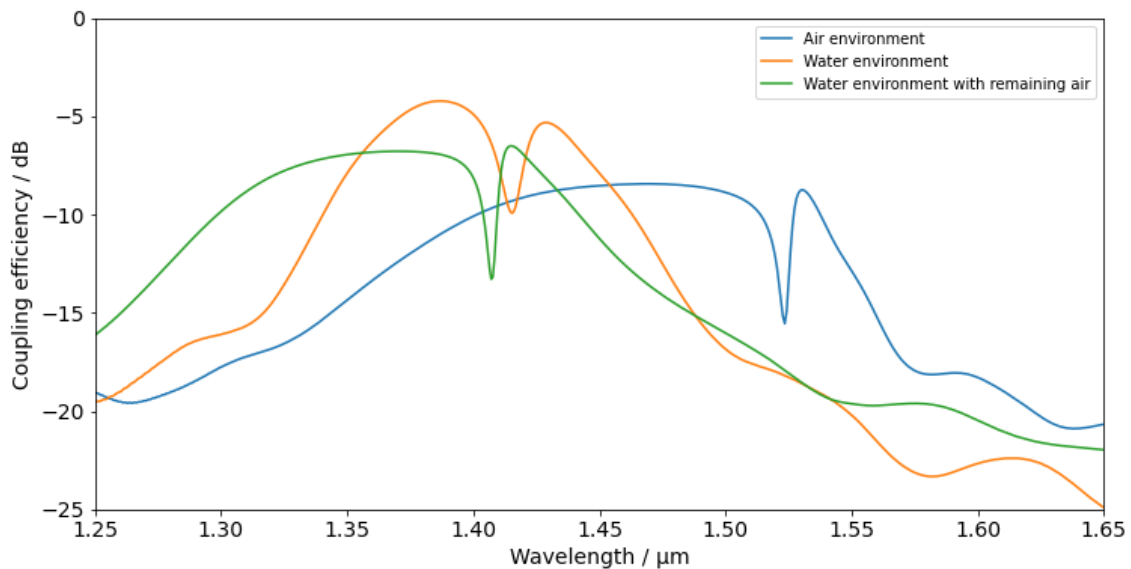


Figure 4: Simulated coupling efficiencies over wavelength for the optimized grating structure in air (blue), in water (orange) and in water where air is still present in the grating trenches (green).

The derived bandwidths are 17 nm, 56 nm and 38 nm for scenarios 1, 2 and 3, respectively. For the latter we observed a decrease of the maximum coupling efficiency and a wavelength shift to 1.41  $\mu\text{m}$ , which is a result of the decreased effective index of the grating mode.

We have to keep in mind that the theoretical target wavelength for the defect mode in the photonic crystal is planned to be 1.53  $\mu\text{m}$  in air and 1.38  $\mu\text{m}$  in water, respectively. But at the time of writing this document we are not able to test these wavelengths yet. So, to be capable of addressing deviating wavelengths, we have to increase the coupler bandwidths.

We therefore introduce a chirp in the grating: different linear chirping methods and went with a linear chirp similar to Dabos et al.<sup>5</sup> where the grating period is linearly changed while the gap width is held constant have been tested.

To find the optimum grating coupler bandwidth while maintaining a high coupling efficiency we tested different chirps in a range from 10 to 50 nm for a varying number of chirped grating periods between 6 and 13 with.

Figures 5, 6 and 7 show the obtained efficiency spectra for different chirps where the optimum number of chirped grating periods was found to be 9 for the first scenario and 8 for the other two and a total number of grating teeth of 22. The first period follows the relation  $\Lambda_1 = \Lambda_{\text{unchirped}} - \text{number of chirped teeth} * \frac{\text{chirp}}{2}$  where for subsequent periods the chirp value was added. From fig. 7 it gets clear that we have to adjust the chirp value of the grating for the third coupling scenario compared to the second in order to achieve a higher coupling efficiency in the desired wavelength region around 1.38  $\mu\text{m}$ .

Table 2 shows the obtained coupling efficiencies for the target wavelengths and -3 dB bandwidths for the chosen grating chirps. We chose the chirps as a compromise between the achieved coupling efficiencies and bandwidths.

Table 2: Simulation results of linear chirped grating optimization for the three described cases.

Case	Target wavelength / $\mu\text{m}$	Optimized chirp / nm	Coupling efficiency at target wavelength / dB	-3 dB bandwidth / nm
1	1.53	50	-9.45	96
2	1.38	10	-5.24	95
3	1.38	40	-7.08	111

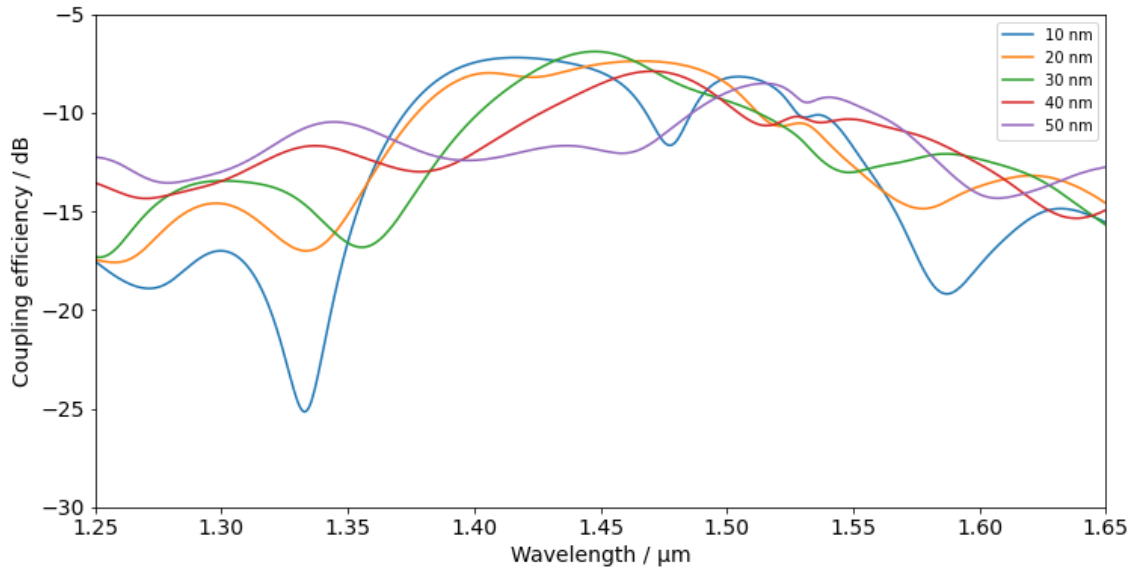


Figure 5: Coupling spectra for different linear grating chirps ranging from 10 to 50 nm for the first coupling scenario.

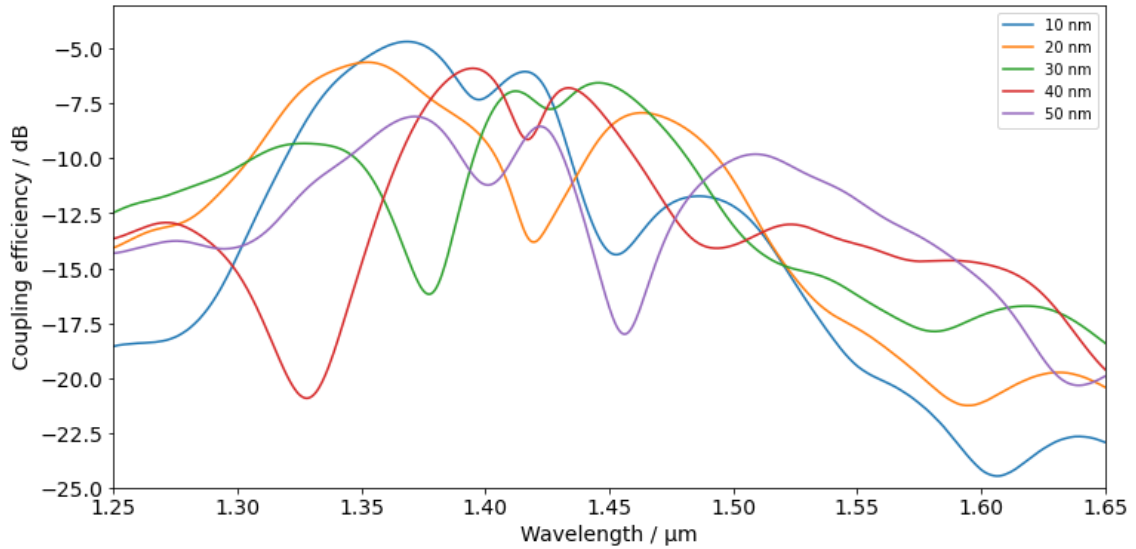


Figure 6: Coupling spectra for different linear grating chirps ranging from 10 to 50 nm for the second coupling scenario.

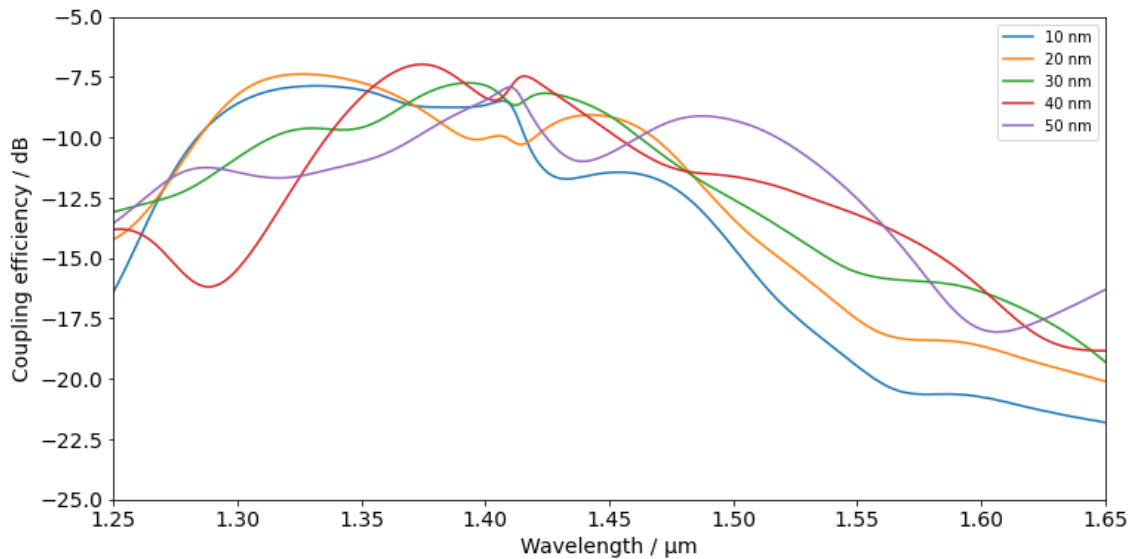


Figure 7: Coupling spectra for different linear grating chirps ranging from 10 to 50 nm for the third coupling scenario.

### 3.2 Design of the adiabatic taper

To convert the mode coming out of a silica single-mode fiber with a diameter of  $10.4 \mu\text{m}$  to the size of the mode of the single-mode SOI waveguide with a cross-section of  $500 \times 400 \text{ nm}^2$  we designed an adiabatic taper. This enables the efficient size conversion of the mode due to a slowly varying waveguide width (taper). Figure 8 shows the transmission through the taper for taper lengths ranging from 10 to 500  $\mu\text{m}$  for structures in air and water respectively. To decide which taper length is needed for the highest conversion efficiency we additionally fitted the function

$$f(L) = T_{max}(1 - \exp(-(L - L_0) * k))$$

to the simulation results, where  $T_{max}$  is the maximum achieved transmission (mode conversion efficiency),  $L$  the taper length with the starting length  $L_0$  and a factor  $k$ . We then defined the needed taper length where the fitted function reaches 99% of the maximum simulated transmission. With this taper design we achieved a theoretical mode conversion efficiency 76% and 78% for a minimum taper length of 300  $\mu\text{m}$  and 330  $\mu\text{m}$  respectively.

To verify these values, we set up a 3D-model in COMSOL with 1  $\mu\text{m}$  thick  $\text{SiO}_2$  under 400 nm thick Si with 1.4  $\mu\text{m}$  air/water on top. The model is shown in figure 9 with a 30  $\mu\text{m}$  long taper for better clarity. In both 3D-simulations we could verify the above found conversion efficiencies for the respective taper lengths of 300  $\mu\text{m}$  and 330  $\mu\text{m}$ .

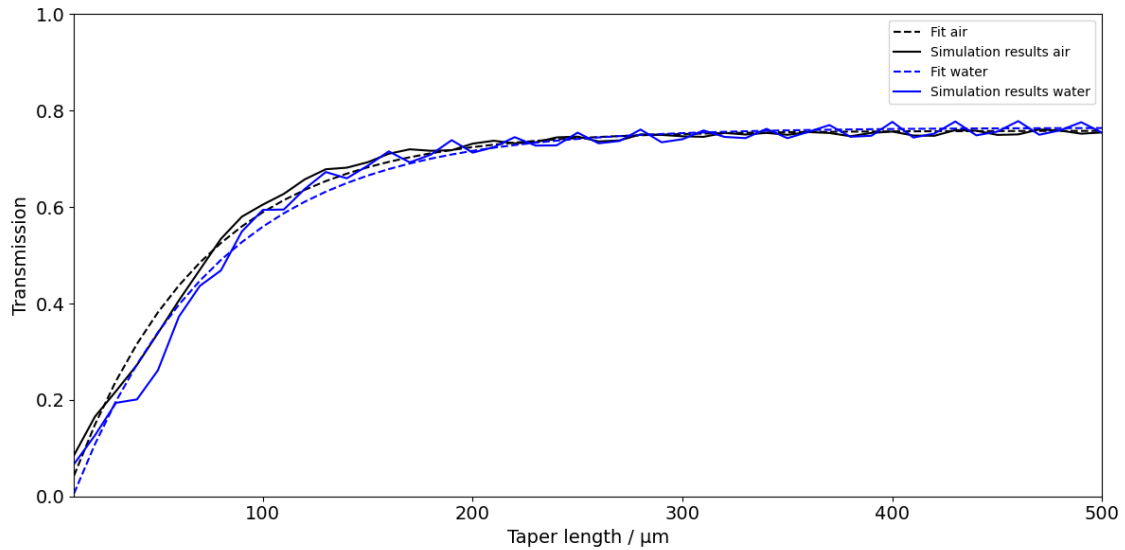


Figure 8: Transmission through the linear taper for operation in air with a target wavelength of 1.53  $\mu\text{m}$  (black) and in water with a target wavelength of 1.38  $\mu\text{m}$  (blue) along with the corresponding fitted curves (dashed lines).

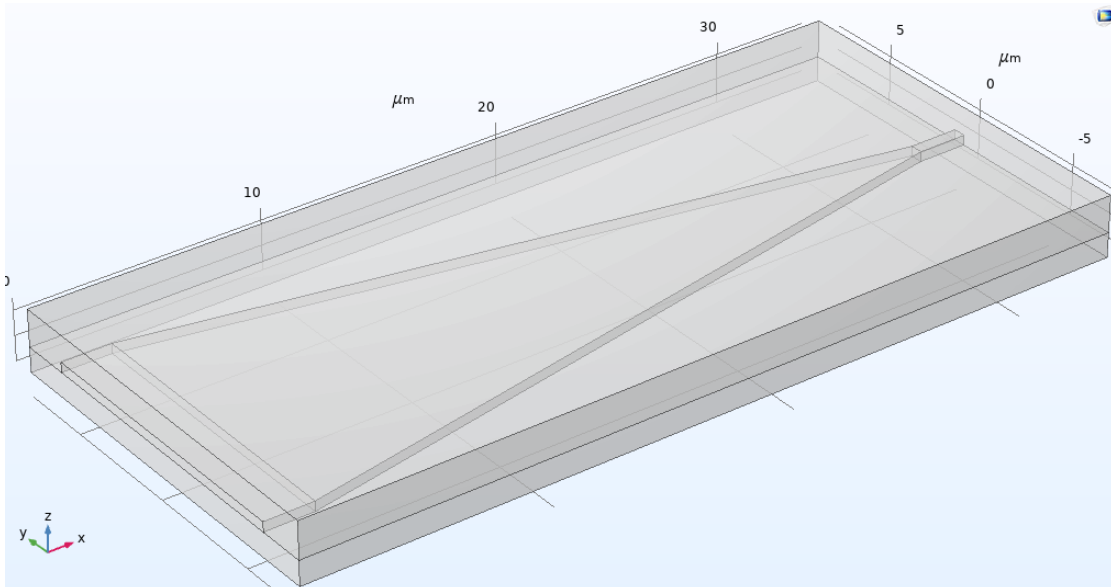


Figure 9: 3D-simulation setup with a taper length of 30  $\mu\text{m}$  for better clarity.

### 3.3 Compatibility with fabrication route

Within the project and to keep the fabrication process as simple as possible, the consortium aims towards a fabrication route, where the pillars and the coupling structures are fabricated in one etching step.

In the following subsection we consider a Si thickness of 400 nm for single-mode operation of the waveguiding structures. If the pillar design requires a modification of the silicon thickness, we will work on this on a later moment.

#### 3.3.1 Influence of variation in Si thickness

Due to the variations of the upper silicon layer that one can encounter on commercial SOI substrates, we have tested the influence of the silicon thickness on the bandwidths and coupling efficiencies in a range from 300 to 500 nm in 10 nm steps for the three earlier described scenarios with the respective chirped geometries.

Figures 10 to 12 show the coupling efficiency spectra. It gets clear that the silicon thickness shifts the wavelength region of efficient coupling. The thinner the silicon the lower the wavelength gets and the thicker the silicon the higher the wavelength, while the -3 dB bandwidth is not influenced significantly. Here, the acceptable thickness deviation is described as where the coupling efficiency at the target wavelength drops by 1 dB compared to the coupling efficiency for Si thickness of 400 nm.

It was found that we can work with a thickness of 380 to 450 nm for the first scenario, 390 to 440 nm for the second scenario and 390 to 430 nm for the third case without drastically altering the coupling efficiency in the desired wavelength region.

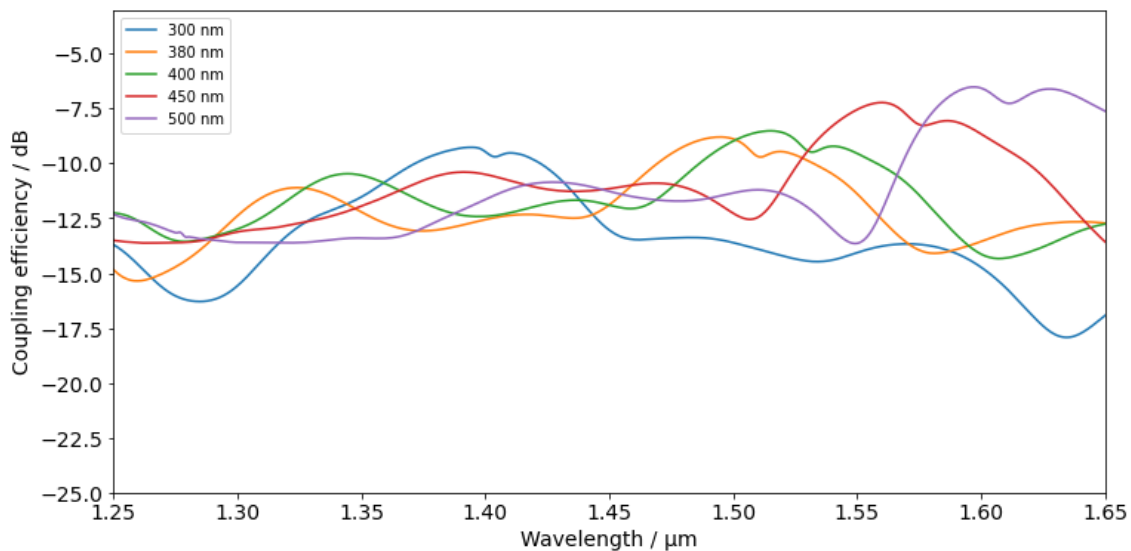


Figure 10: Coupling spectra for different Si thicknesses of the expected case with 400 nm thickness, the thicknesses of the lower and upper limits and thicknesses of 300 nm and 500 nm respectively for the first coupling scenario.

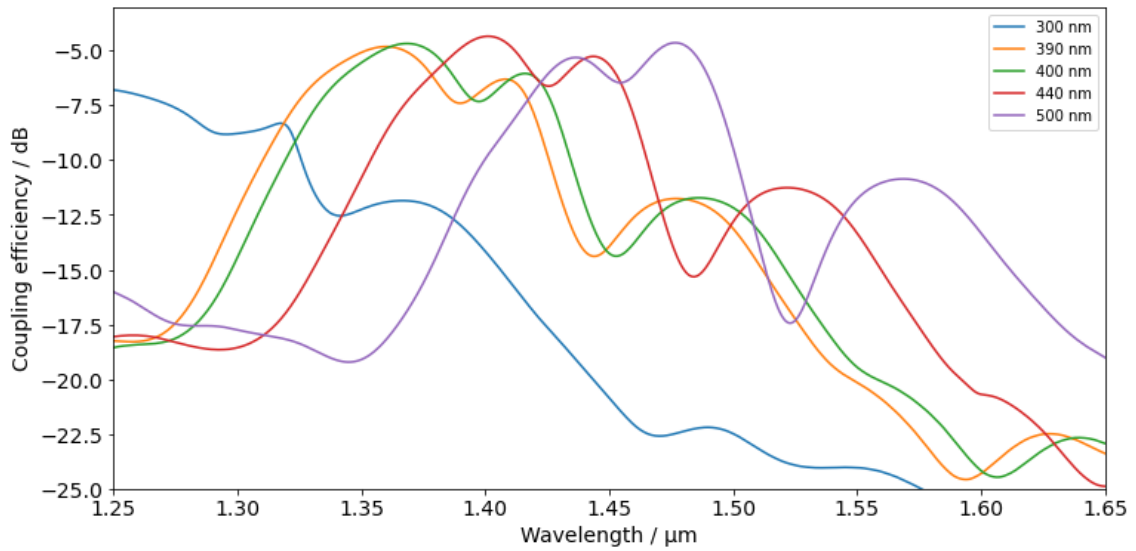


Figure 11: Coupling spectra for different Si thicknesses of the expected case with 400 nm thickness, the thicknesses of the lower and upper limits and thicknesses of 300 nm and 500 nm respectively for the second coupling scenario.

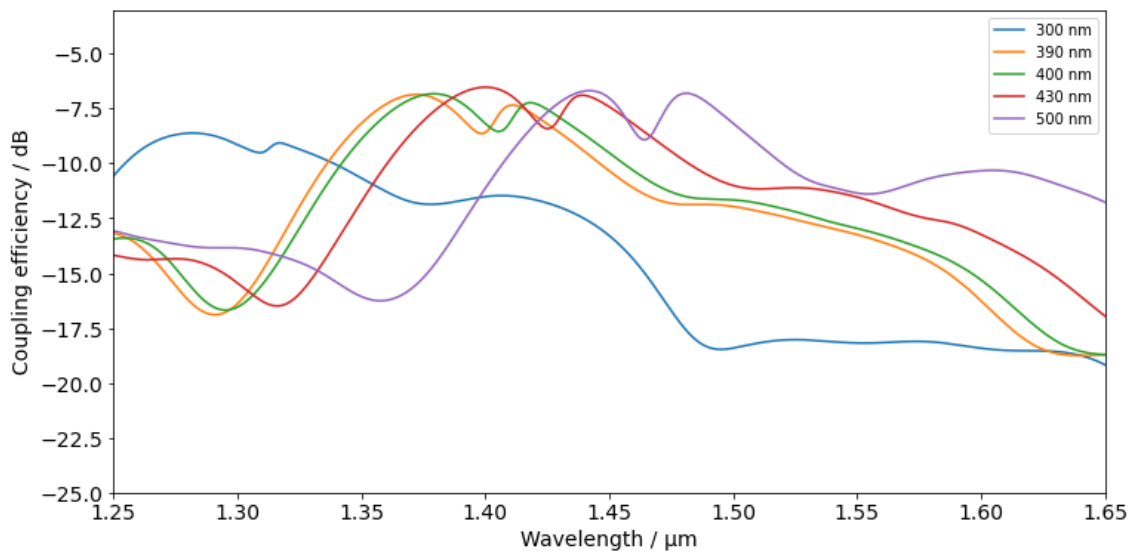


Figure 12: Coupling spectra for different Si thicknesses of the expected case with 400 nm thickness, the thicknesses of the lower and upper limits and thicknesses of 300 nm and 500 nm respectively for the third coupling scenario.

## 4 Conclusions and future work

---

In this report, we present the simulation and modeling for the design of one-dimensional grating couplers for the operation in air with a target wavelength of 1.53  $\mu\text{m}$  and in water with a target wavelength of 1.38  $\mu\text{m}$  to couple light from a single-mode silica fiber to a single-mode waveguide on a SOI platform. The choice of these wavelengths results from simulations of the photonic crystal, where the wavelengths of the introduced defect modes lie in these specific regions. To allow fabrication adjustments of the physical device, we also optimized the bandwidth of the couplers to be more flexible towards the central wavelength used. These figures will be meaningful for the later development of StretchBio devices.

To address the high mode-field mismatch of the fiber mode and the waveguide mode we have designed a linear adiabatic taper for efficient mode-field conversion.

The simulations have shown that the coupling efficiency of the optimized gratings in air is overall lower than in water. This fact results from a poorer phase matching in air due to a larger refractive index difference of the grating to the surrounding medium.

The here presented simulation results provide important design parameters for the fabrication of the actual coupler device and information on how we can adapt the fabrication strategy to be compatible with the fabrication of the photonic crystal.

In the later steps of the StretchBio project, we will work with living tissue. Therefore, we expect the structures to be in watery environment. As mentioned before, due to the dimensions of the grating trenches, we expect them to be filled with air. So, the grating design for the third coupling scenario is the most promising to work with in the upcoming months.

The thickness of the grating structures and the subsequent waveguides might not match the height of the photonic crystals, as previously described in the deliverable D3.1. Considering this, further investigations will be carried out to test the coupling between the waveguide structures and the photonic crystal.

## Glossary

---

Abbreviation	Explanation
nm	Nanometers
$\mu\text{m}$	Micrometers
$\text{SiO}_2$	Silicon dioxide
Si	Silicon
WP	Work package
TM	Transverse magnetic
SOI	Silicon on insulator
FDTD	Finite-difference-time-domain